



Synthesis, crystal structure and luminescence properties of lanthanide complexes with a new semirigid bridging furfurylsalicylamide ligand

Xue-Qin Song^{a,*}, Li Wang^a, Qing-Fang Zheng^a, Wei-Sheng Liu^{b,*}

^a School of Chemical and Biological Engineering, Lanzhou Jiaotong University, Lanzhou 730070, China

^b College of Chemistry and Chemical Engineering and State Key Laboratory of Applied Organic Chemistry, Lanzhou University, Lanzhou 730000, China

ARTICLE INFO

Article history:

Received 4 February 2012

Received in revised form 3 April 2012

Accepted 3 April 2012

Available online 23 April 2012

Keywords:

Salicylamide ligand

Lanthanide coordination polymer

Crystal structure

Luminescence properties

ABSTRACT

We present here new lanthanide coordination polymers based on a semirigid bridging furfurylsalicylamide ligand which were synthesized and characterized by elemental analysis, X-ray powder diffraction and IR measurements. The coordination polymer $[\text{Pr}_2\text{L}_3(\text{NO}_3)_6]_\infty$ displays a two-dimensional honeycomb-like framework, which can be regarded as a (6,3) topological network with praseodymium atoms acting as “three-connected” centers. The photoluminescence analysis indicates that there is an efficient ligand-to-Ln(III) energy transfer in Tb(III) complex and the ligand is an efficient “antenna” for Tb(III). From a more general perspective, the results demonstrated herein provide the possibility of controlling the formation of the desired lanthanide coordination structure to enrich the crystal engineering strategy and enlarges the arsenal for developing excellent luminescent lanthanide complexes of salicylamide derivatives.

© 2012 Published by Elsevier B.V.

1. Introduction

Materials incorporating lanthanide ions are of great interest for a wide range of optical applications, such as biomedical analysis and material science [1,2]. Trivalent lanthanide ions are fascinating in luminescence sources for their high color purity and relatively long lifetimes of the excited states. Among the luminescent lanthanide complexes, Eu(III) and Tb(III) compounds show strong luminescence in the visible region, making them to be good candidates for fluoroimmunoassays and structural probes. Lanthanide ions exhibit, however, low luminescence intensity due to the fact that the $4f \rightarrow 4f$ transitions are parity forbidden. One of the most useful strategies that has been employed to overcome this drawback is to combine the lanthanide ions through the coordination with organic ligands acting as sensitizers, which is the so-called “antenna effect” [3,4]. The ligands absorb UV or visible light and efficiently transfer the energy to the central lanthanide ion (intramolecular energy transfer), ultimately resulting in sensitized Ln(III) ion emission. Among the various organic ligands [5–10] used for constructing lanthanide coordination complexes, salicylamide derivatives provide a fascinating prospect in preparing lanthanide coordination polymers possessing strong luminescence properties [11] which prompts us to synthesize and investigate analogs of the extensive series of these ligands. Therefore we synthesis the new member of salicylamide derivatives namely, 3,6-bis[(2'-

furfurylaminoformyl)phenoxy]methyl}-1,2,4,5-tetramethylbenzene (**L**) (Scheme 1) and the resulting lanthanide complexes to extend our systematic research.

As a result, the reaction of **L** with trivalent lanthanide ions afforded a novel two-dimensional honeycomb-like framework, which can be regarded as a (6,3) topological network with praseodymium atoms acting as “three-connected” centers. Under the excitation of UV light, Sm(III), Eu(III), Tb(III) and Dy(III) complexes exhibit characteristic emissions of corresponding lanthanide ions. The lowest triplet state energy levels of the ligand was calculated from the phosphorescence spectra of the Gd(III) complex at 77 K. The results presented herein indicated that the new semirigid bridging ligand exhibited a good antennae effect with respect to the Tb(III) ion due to efficient intersystem crossing and ligand to metal energy transfer.

2. Experimental

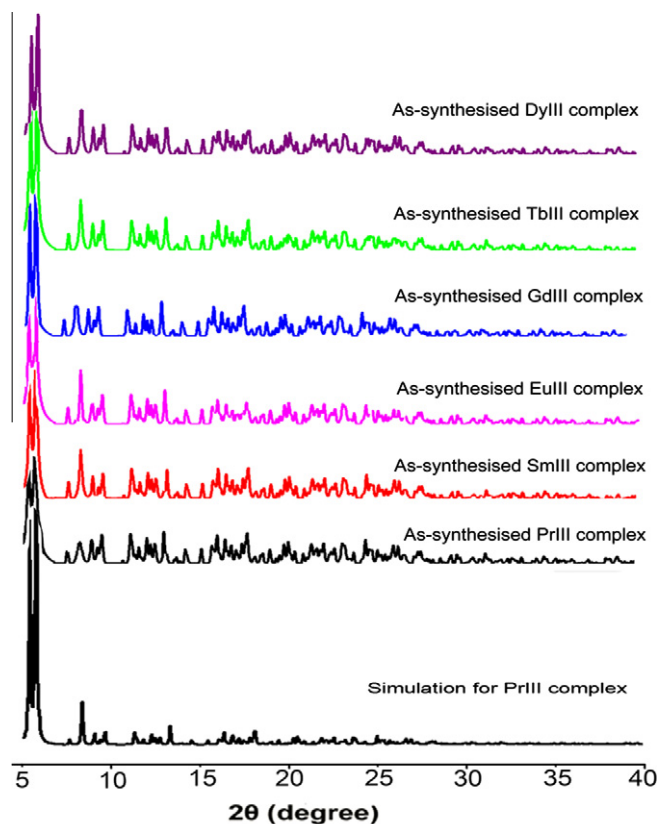
2.1. Materials and instrumentation

Furfurylamine was obtained from Alfa Aesar Co. Other commercially available chemicals were of analytical grade and were used without further purification. The lanthanide nitrates [12] were prepared according to the literature method.

The metal ions were determined by EDTA titration using xylene orange as indicator. Carbon, nitrogen and hydrogen analyses were performed using an EL elemental analyzer. Melting points were determined on a Kofler apparatus. Powder X-ray diffraction patterns (PXRD) were determined with Rigaku-D/Max-II X-ray diffractometer with graphite-monochromatized Cu K α radiation.

* Corresponding authors. Tel.: +86 931 8843385; fax: +86 931 4938755 (X.-Q. Song), tel./fax: +86 931 8915151 (W.-S. Liu).

E-mail addresses: songxq@mail.lzjtu.cn (X.-Q. Song), liuws@lzu.edu.cn (W.-S. Liu).



Scheme 1. The synthetic route of the ligand L.

Infrared spectra ($4000\text{--}400\text{ cm}^{-1}$) were obtained with KBr discs on a Thermo Mattson FTIR spectrometer. ^1H NMR spectra were recorded on a Bruker DRX 300 spectrometer in CDCl_3 solution with TMS as internal standard. Fluorescence measurements of the well grinded thick solid samples were made on a Hitachi F-4500 spectrophotometer equipped with a xenon lamp as the excitation source (front-face mode). Samples were placed between two quartz cover slips and the excitation and emission slit of 2.5 nm were used. The 77 K solution-state phosphorescence spectra of the Gd(III) complex was recorded with solution samples (a 1:1 ethyl acetate–MeOH (v/v) mixture) loaded in a quartz tube inside a quartz-walled optical Dewar flask filled with liquid nitrogen in the phosphorescence mode [13]. Quantum yields were determined by an absolute method [14] using an integrating sphere on FLS920 of Edinburgh Instrument. The luminescence decays were recorded using a pumped dye laser (Lambda Physics model FL2002) as the excitation source. The nominal pulse width and the line width of the dye-laser output were 10 ns and 0.18 cm^{-1} , respectively. The emission of the sample was collected by two lenses in a monochromator (WDG30), detected by a photomultiplier and processed by a Boxcar Average (EGG model 162) in line with a microcomputer. Reported quantum yields and luminescence lifetimes are averages of at least three independent determinations. The estimated errors for quantum yields and luminescence lifetimes are 10%.

2.2. Synthesis of the ligand

The synthetic route for the ligand (L) is shown in Scheme 1. 2-furfurylsalicylamide was prepared according to the literature procedure with minor modifications [15] and 1,4-bis(bromomethyl)-2,3,5,6-tetramethylbenzene [16] were prepared according to the literature.

Table 1

Crystal data and structure refinement parameters for Pr(III) complex.

Empirical formula	$\text{C}_{108}\text{H}_{108}\text{N}_{12}\text{O}_{36}\text{Pr}_2$
Crystal system, space group	Triclinic, $P-1$
Unit cell dimensions	
a (Å)	11.729(6)
b (Å)	17.716(9)
c (Å)	20.360(10)
α (°)	69.109(6)
β (°)	89.186(6)
γ (°)	89.739(7)
V (Å ³)	3952(3)
Z , Calculated density (kg/m^3)	1, 1.021
Absorption coefficient (mm^{-1})	0.671
$F(000)$	1244
Crystal size (mm)	$0.46 \times 0.45 \times 0.31$
Theta range for data collect (°)	2.03–25.01
Limiting indices	$-13 \leq h \leq 13$, $-21 \leq k \leq 16$, $-24 \leq l \leq 24$
Reflections collected/unique	20017/13537 [$R(\text{int}) = 0.0631$]
Completeness to theta = 25.01 (%)	97.2
Data/restraints/parameters	13537/2/712
Goodness-of-fit on F^2	1.000
Final R indices [$I > 2\sigma(I)$]	$R_1 = 0.0751$, $wR_2 = 0.1580$
R indices (all data)	$R_1 = 0.1405$, $wR_2 = 0.1685$

To a solution of 2-furfurylsalicylamide (2.28 g, 10.5 mmol) in dry acetone was added 1.52 g (11 mmol) dried K_2CO_3 , and the mixture was stirred for 30 min at room temperature, 1.59 g (5 mmol) 1,4-bis(bromomethyl)-2,3,5,6-tetramethylbenzene in 20 ml of dry acetone was added dropwise in 30 min and the resulting solution stirred and heated to reflux for 24 h. After cooling down, inorganic salts were separated by filtration and the solvent removed from the filtrate under reduced pressure. The crude product was recrystallized with ethyl acetate to give a white solid. 2.55 g, Yield 86%. M.p. 151–152 °C. *Anal. Calc.* for $\text{C}_{36}\text{H}_{36}\text{N}_2\text{O}_6$: C, 72.95; H, 6.12; N, 4.73. Found: C, 72.67; H, 6.14; N, 4.76%. IR (KBr, ν , cm^{-1}): 3375 (s), 2912 (m), 2886 (w), 1645 (s, C=O), 1597 (m), 1532 (s), 1481 (m), 1293 (s), 1226 (s, Ar–O), 752 (s). ^1H NMR (CDCl_3 , 300 MHz): δ : 2.25 (s, 12H, CH_3), 4.41 (d, 4H, NHCH_2 , $J = 3.6$ Hz), 5.25 (s, 4H, OCH_2), 5.80 (d, 2H, furan d, $J = 2.7$ Hz), 6.13 (m, 2H, furan d, $J = 2.1$ Hz), 7.09–7.54 (m, 6H, ArH), 7.53 (t, 2H, Ar, $J = 5.4$ Hz), 8.11 (t, 2H, NH), 8.31 (d, 2H, Ar, $J = 6.9$ Hz).

2.3. Synthesis of the complexes

To a clear solution of L (0.086 g, 0.1 mmol) in CHCl_3 (2 ml) was added $\text{Ln}(\text{NO}_3)_3 \cdot 5\text{H}_2\text{O}$ (0.15 mmol) in 10 ml of ethyl acetate. The resulting solution was left stirring overnight at room temperature to afford a pale white solid which was filtered off, washed three times with ethyl acetate and CHCl_3 respectively, and dried over CaCl_2 for 3 days to give the product in 70–80% yield. The single crystals of Pr(III) complex were obtained as follows: 10 ml of ethyl acetate was added to a clear solution of L (0.086 g, 0.1 mmol) in CHCl_3 (2 ml) in 30 ml test tube. The resulting solution was left standing for about 30 min, then $\text{Pr}(\text{NO}_3)_3 \cdot 5\text{H}_2\text{O}$ (0.15 mmol) in 10 ml of ethyl acetate was added carefully and sealed for crystallization at room temperature. After about two weeks pale green crystals suitable for analysis were obtained.

2.4. X-ray single-crystal diffraction analysis

Structure diffraction intensities for Pr(III) complex were carried out on a Bruker SMART Apex CCD area detector diffractometer (Mo $\text{K}\alpha$, $\lambda = 0.71073$ Å) at 293 K. Lorentz-polarization and absorption corrections were applied for the compound. The structure was solved with direct methods and refined with full-matrix

Table 2
Selected bond lengths (Å) and angles (°) for Pr(III) complex.

Pr(1)–O(8)	2.393(6)	Pr(1)–O(5)	2.396(5)	Pr(1)–O(2)	2.422(5)	Pr(1)–O(11)	2.535(7)
Pr(1)–O(17)	2.541(6)	Pr(1)–O(16)	2.544(6)	Pr(1)–O(13)	2.546(6)	Pr(1)–O(10)	2.551(6)
Pr(1)–O(14)	2.555(8)						
O(8)–Pr(1)–O(5)	77.0(2)	O(8)–Pr(1)–O(2)	87.8(2)	O(5)–Pr(1)–O(2)	146.3(3)	O(5)–Pr(1)–O(11)	123.5(2)
O(8)–Pr(1)–O(11)	82.7(3) 77.8(8)	O(5)–Pr(1)–O(11)	146.3(3)	O(2)–Pr(1)–O(11)	123.5(2)	O(2)–Pr(1)–O(17)	160.40(18)
O(8)–Pr(1)–O(17)	81.8(2) 118.7(6)	O(5)–Pr(1)–O(17)	78.9(2)	O(2)–Pr(1)–O(17)	160.40(18)	O(5)–Pr(1)–O(16)	101.8(2)
O(11)–Pr(1)–O(17)	71.8(3)	O(8)–Pr(1)–O(16)	128.4(2)	O(5)–Pr(1)–O(16)	101.8(2)	O(17)–Pr(1)–O(16)	48.5(2)
O(2)–Pr(1)–O(16)	143.7(2)	O(11)–Pr(1)–O(16)	70.6(3)	O(17)–Pr(1)–O(16)	48.5(2)	O(2)–Pr(1)–O(13)	78.6(2)
O(8)–Pr(1)–O(13)	153.2(2)	O(5)–Pr(1)–O(13)	123.2(3)	O(2)–Pr(1)–O(13)	78.6(2)	O(16)–Pr(1)–O(13)	68.8(2)
O(11)–Pr(1)–O(13)	85.6(3)	O(17)–Pr(1)–O(13)	117.2(2)	O(16)–Pr(1)–O(13)	68.8(2)	O(2)–Pr(1)–O(10)	75.3(2)
O(8)–Pr(1)–O(10)	78.3(2)	O(5)–Pr(1)–O(10)	147.2(2)	O(16)–Pr(1)–O(10)	110.4(2)	O(5)–Pr(1)–O(14)	74.3(2)
O(11)–Pr(1)–O(10)	48.3(2)	O(17)–Pr(1)–O(10)	118.4(2)	O(5)–Pr(1)–O(14)	74.3(2)	O(17)–Pr(1)–O(14)	102.1(2)
O(13)–Pr(1)–O(10)	76.0(3)	O(8)–Pr(1)–O(14)	149.5(2)	O(17)–Pr(1)–O(14)	102.1(2)	O(10)–Pr(1)–O(14)	123.2(2)
O(2)–Pr(1)–O(14)	78.7(2) 130.23(11)	O(11)–Pr(1)–O(14)	127.4(3)				
O(16)–Pr(1)–O(14)	68.2(2)	O(13)–Pr(1)–O(14)	49.7(2)				

least squares on F^2 using the SHELXL-97 program package [17]. All non-hydrogen atoms were subjected to anisotropic refinement, and all hydrogen atoms were added in idealized positions and refined isotropically. Crystal data and details of the refinement are summarized in Table 1, representative bond lengths (Å) and angles (°) are presented in Table 2. CCDC reference numbers 863911.

3. Results and discussion

3.1. Physical measurements

Analytical data for the newly synthesized complexes, listed in Table 3, conforms to a 2:3 metal-to-L stoichiometry for nitrate complexes. All complexes are soluble in DMF, DMSO, ethanol, methanol and slightly soluble in ethyl acetate. The molar conductance of the complexes in methanol (see Table 3) indicate that all complexes act as non-electrolytes.

As shown in Table 4 and Fig. 1, the characteristic band of carbonyl group of free ligand **L** is shown at 1645 cm^{-1} . The absence of the band round 1645 cm^{-1} which is instead of a new band at ca 1611 cm^{-1} of the complex compared to the free ligand indicates

the complete coordination of the ligand. Weak absorptions observed in the range of $2900\text{--}2950\text{ cm}^{-1}$ can be attributed to the ν_{CH_2} of the ligand. The absorption bands assigned to the coordinated nitrates were observed as two group bands at about 1484 cm^{-1} (ν_1) and 1295 cm^{-1} (ν_4) for the complexes. The differences between the strongest absorption band ν_1 and ν_4 of nitrate group lie in ca 180 cm^{-1} , indicating that coordinated nitrate groups in the complexes are bidentate ligands [18], the ν_3 of free nitrate group disappears in the spectra of the complexes which is in agreement with the results of the conductivity experiment, implying that three nitrate groups are all in coordination sphere. The room temperature PXRD patterns of the PrIII, SmIII, EuIII, GdIII, TbIII, DyIII complexes with the ligand **L** as well as that of simulation for PrIII complex single crystal are unfolded from 5° to 40° as shown in Fig. 2. According to the elemental analysis, IR and PXRD, complexes of the ligand have similar coordination structure with PrIII complex.

3.2. Crystal structure descriptions

The structure comprises of a covalently bonded two-dimensional (2D) honeycomb of composition $[\text{Pr}_2(\text{NO}_3)_6\text{L}_3]_\infty$ crystallized

Table 3
Analytical and molar conductance data for the complexes (calculated values in parentheses).

Complex	Elemental Analysis (%) ^a				$\Lambda_m(\Omega^{-1}\text{cm}^2\text{mol}^{-1})$
	C	H	N	Ln	
$\text{Pr}_2\text{L}_3(\text{NO}_3)_6$	53.18 (53.34)	4.46 (4.48)	6.94 (6.91)	11.54 (11.59)	68.4
$\text{Sm}_2\text{L}_3(\text{NO}_3)_6$	53.11 (53.19)	4.45 (4.46)	6.86 (6.89)	11.79 (11.83)	73.9
$\text{Eu}_2\text{L}_3(\text{NO}_3)_6$	52.74 (52.86)	4.42 (4.44)	6.88 (6.85)	12.44 (12.38)	65.8
$\text{Gd}_2\text{L}_3(\text{NO}_3)_6$	52.54 (52.63)	4.43 (4.42)	6.79 (6.82)	12.69 (12.76)	72.3
$\text{Tb}_2\text{L}_3(\text{NO}_3)_6$	52.67 (52.56)	4.40 (4.41)	6.80 (6.81)	12.83 (12.88)	75.5
$\text{Dy}_2\text{L}_3(\text{NO}_3)_6$	52.26 (52.41)	4.38(4.40)	6.76 (6.79)	13.05 (13.13)	74.8

^a Data in parentheses are calculated values.

Table 4
The most important IR bands for the lanthanide nitrate complexes(cm^{-1}).

Compound	$\nu(\text{C}=\text{O})$	$\nu(\text{C}-\text{O}-\text{C})$	$\nu_1(\text{NO}_3^-)$ (NO_3^-) (NO_3^-)	$\nu_4(\text{NO}_3^-)$	$\nu_2(\text{NO}_3^-)$	$\nu_3(\text{NO}_3^-)$	$ \nu_1-\nu_4 $
L	1645	1226	–	–	–	–	–
$\text{Pr}_2\text{L}_3(\text{NO}_3)_6$	1611	1224	1484	1295	1029	816	189
$\text{Sm}_2\text{L}_3(\text{NO}_3)_6$	1610	1221	1485	1303	1028	815	182
$\text{Eu}_2\text{L}_3(\text{NO}_3)_6$	1611	1224	1479	1300	1029	817	179
$\text{Gd}_2\text{L}_3(\text{NO}_3)_6$	1611	1222	1482	1303	1028	817	179
$\text{Tb}_2\text{L}_3(\text{NO}_3)_6$	1611	1223	1484	1300	1033	816	184
$\text{Dy}_2\text{L}_3(\text{NO}_3)_6$	1612	1222	1484	1302	1020	815	182

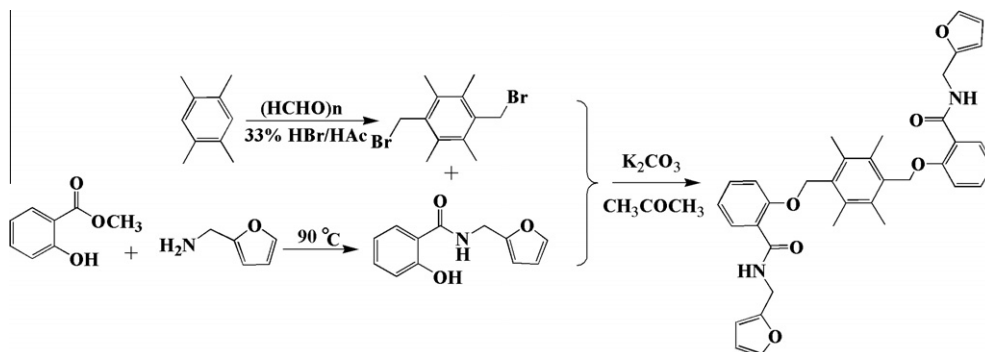


Fig. 1. IR Spectra of ligand **L** (solid line) and its Tb(III) complex in solid state.

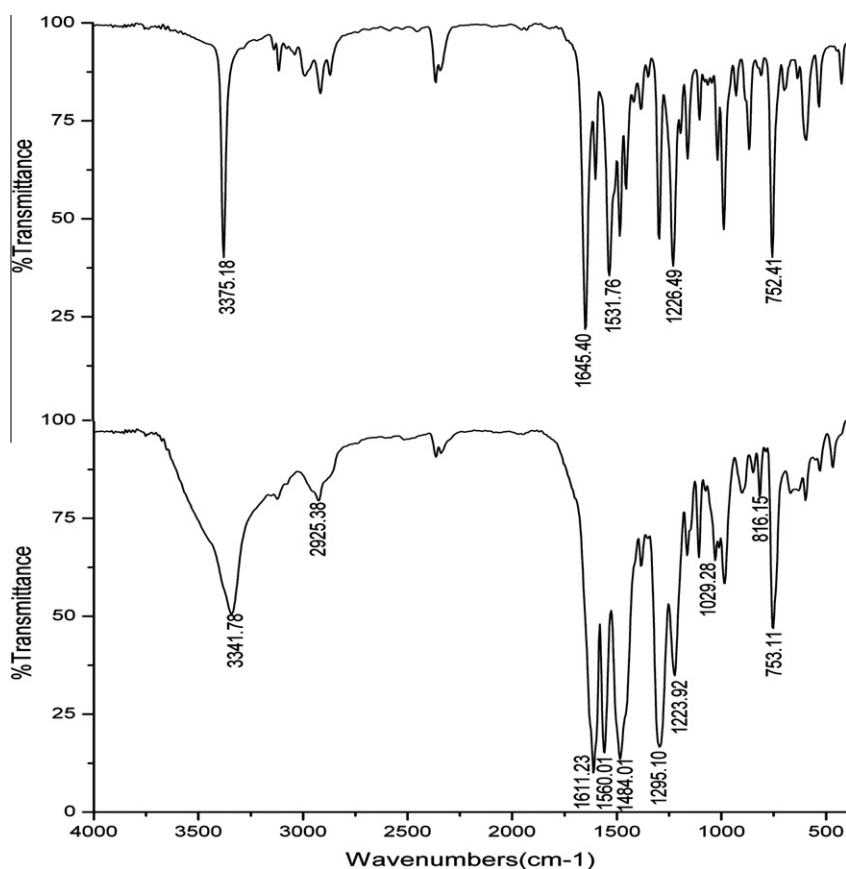


Fig. 2. Powder x-ray diffraction patterns of complexes.

in the triclinic $P\bar{1}$ space group which is quite different from the structure of Pr(III) complex reported recently [11g]. As shown in Fig. 3, each Pr(III) node lies in a distorted monocapped square antiprism coordination sphere, which is defined by three carbonyl oxygen and six nitrate oxygen donors with Pr–O distances range from 2.393(5) to 2.555(7) Å. The two carbonyl oxygens of the same ligand are coordinated to the two different Pr(III) ion in a trans configuration. Each praseodymium center, shown as green large spheres in Fig. 4, connects three ligands, While, each ligand molecule is connected to two praseodymium atoms. The combination of bridging **L** and nona-coordinated praseodymium atoms build up a two-dimensional honeycomb-like framework in the *ab* plane, which can be regarded as a (6,3) topological network with praseodymium atoms acting as “three-connected” centers (Fig. 4).

3.3. Luminescence properties

Upon UV irradiation, the free ligand emits a strong blue luminescence (λ_{\max} at ca. 455 nm) that can be easily detected with naked eyes. However, upon complexation with trivalent lanthanide this emission is replaced by the typical luminescent color arising from Ln(III) cation. The luminescence characteristics of the ligand and lanthanide complexes in solid state were measured at room temperature under identical experimental conditions, and the luminescence data in solid state are listed in Table 5.

For the Sm(III) complex of **L**, the emission intensity is the weakest, but two characteristic bands can still be observed. They were attributed to $^4G_{5/2} \rightarrow ^6H_J$ ($J = 5/2, 7/2$) transitions (Fig. 5). The solid state excitation and emission spectrum of europium complex of **L**

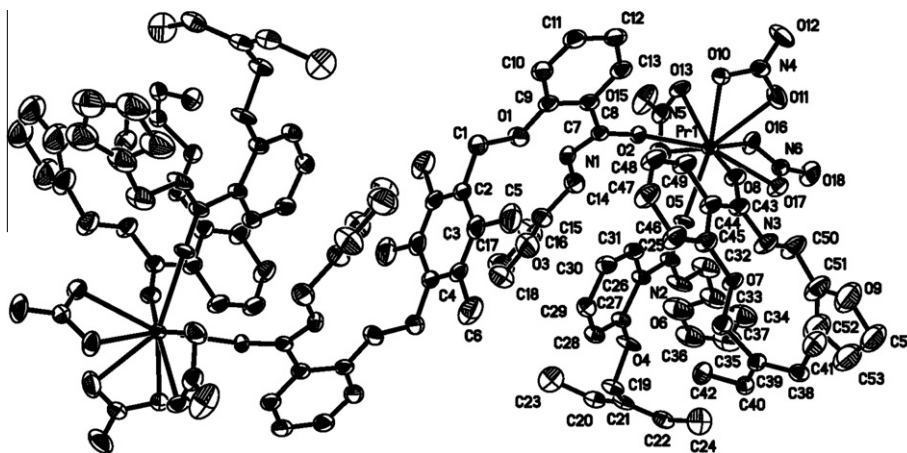


Fig. 3. ORTEP plot of Pr(III) complex showing the local coordination environment with thermal ellipsoids at 30% probability (hydrogen atoms are omitted for clarity).

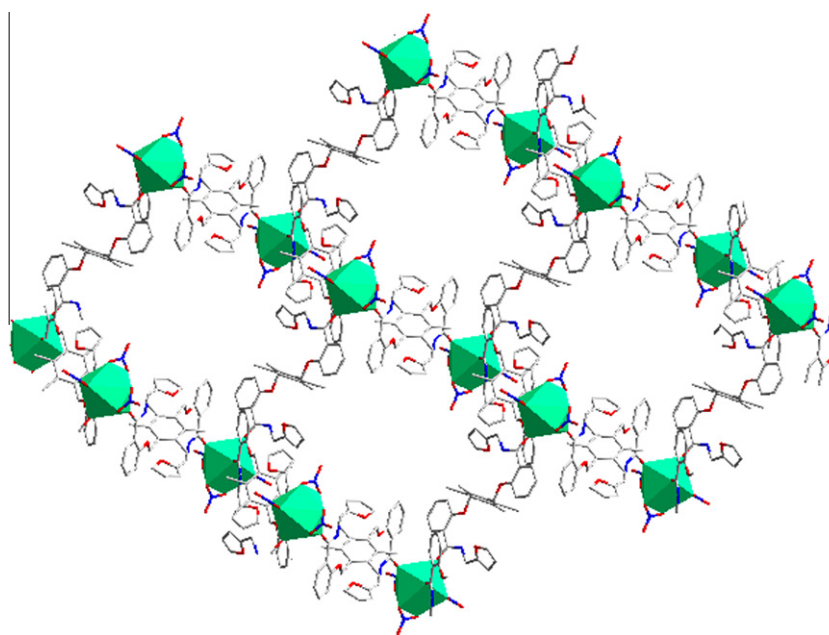


Fig. 4. 2D honeycomb coordination polymer of $[\text{Pr}_2\text{L}_3(\text{NO}_3)_6]_\infty$ (hydrogen atoms are omitted for clarity).

Table 5

Luminescence data for the ligand and its complexes.

	Slit (nm)	λ_{ex} (nm)	λ_{em} (nm)	RFI	Assignment	τ (ms) ^a	$\Phi\%$ ^a
$\text{Sm}_2\text{L}_3(\text{NO}_3)_6$	2.5	319	563	56.77	$^4\text{G}_{5/2} \rightarrow ^6\text{H}_{5/2}$	0.043	–
			598	74.7	$^4\text{G}_{5/2} \rightarrow ^6\text{H}_{7/2}$		
$\text{Eu}_2\text{L}_3(\text{NO}_3)_6$	2.5	397	580	12.55	$^5\text{D}_0 \rightarrow ^7\text{F}_0$	0.314	0.49
			593	76.59	$^5\text{D}_0 \rightarrow ^7\text{F}_1$		
			618	187.5	$^5\text{D}_0 \rightarrow ^7\text{F}_2$		
$\text{Tb}_2\text{L}_3(\text{NO}_3)_6$	2.5	320	492	376.4	$^5\text{D}_4 \rightarrow ^7\text{F}_6$	0.926	2.4
			546	1325	$^5\text{D}_4 \rightarrow ^7\text{F}_5$		
			583	87.5	$^5\text{D}_4 \rightarrow ^7\text{F}_4$		
$\text{Dy}_2\text{L}_3(\text{NO}_3)_6$	2.5	320	457	4.53	$^4\text{I}_{15/2} \rightarrow ^6\text{H}_{15/2}$	0.069	–
			482	128.5	$^4\text{F}_{9/2} \rightarrow ^6\text{H}_{15/2}$		
			573	125.7	$^4\text{F}_{9/2} \rightarrow ^6\text{H}_{13/2}$		

^a Luminescence lifetimes and quantum yield values are reported here with an error of $\pm 10\%$.

at room temperature is shown in Fig. 6 and Fig. 7 respectively. The excitation spectrum of europium complex of **L** exhibited a series of sharp lines characteristic of the Eu(III) energy-level structure and assigned to transitions between the $^7\text{F}_{0,1}$ and $^5\text{L}_6$, $^5\text{D}_2$ levels [19],

which indicates that the Eu(III) luminescence is not efficiently sensitized by the ligand which is similar to those reported previously [11]. There were four characteristic peaks of Eu(III) shown in the emission spectra, which were attributed to $^5\text{D}_0 \rightarrow ^7\text{F}_0$ (580 nm),

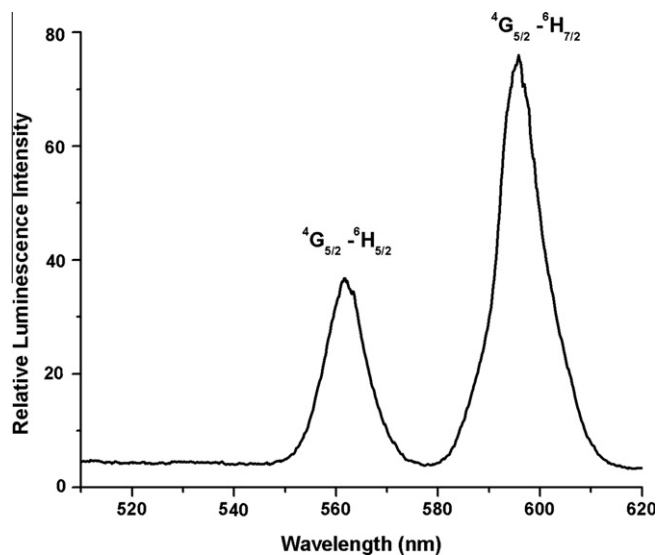


Fig. 5. Room-temperature emission spectra for samarium complex of ligand L ($\lambda_{\text{ex}} = 319$ nm, excitation and emission passes = 2.5 nm) in the solid state.

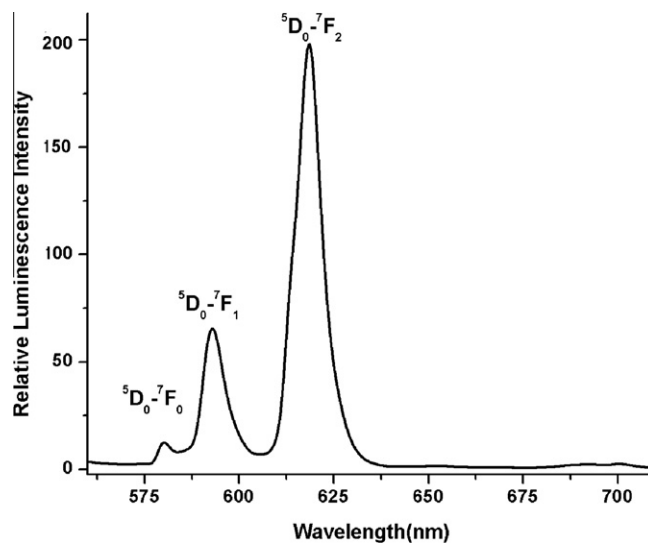


Fig. 7. Room-temperature emission spectra for europium complex of ligand L ($\lambda_{\text{ex}} = 397$ nm, excitation and emission passes = 2.5 nm) in the solid state.

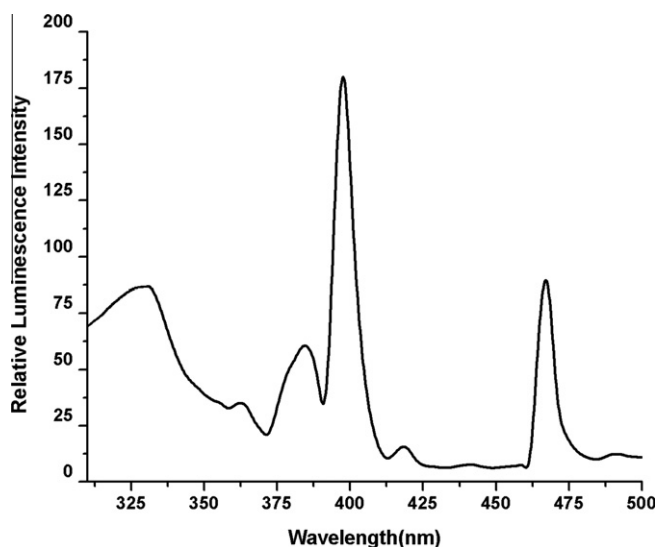


Fig. 6. Room-temperature excitation spectra for europium complex of ligand L with emission monitored at approximately 619 nm (excitation and emission passes = 2.5 nm) in the solid state.

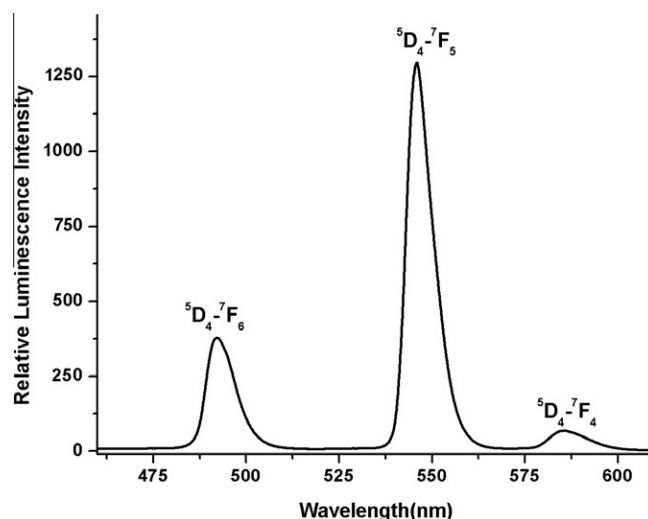


Fig. 8. Room-temperature emission spectra for terbium complex of ligand L ($\lambda_{\text{ex}} = 320$ nm, excitation and emission passes = 2.5 nm) in the solid state.

$^5D_0 \rightarrow ^7F_1$ (593 nm), $^5D_0 \rightarrow ^7F_2$ (619 nm) and $^5D_0 \rightarrow ^7F_4$ (689 nm). The sharpness of the nondegenerate transition ($^5D_0 \rightarrow ^7F_0$) indicates that all the Eu(III) coordinated in the sample have essentially identical ligand coordination and structural environments. The intensity of the $^5D_0 \rightarrow ^7F_2$ transition (electric dipole) is stronger than that of the $^5D_0 \rightarrow ^7F_1$ transition (magnetic dipole), indicating that the coordination environment of the Eu(III) ion is asymmetric [20]. For Tb(III) complex, the emission intensity is stronger than that of the other three complex in the same experimental conditions. Four characteristic peaks are shown in Fig. 8, assigned to the $^5D_4 \rightarrow ^7F_J$ ($J = 3, 4, 5, 6$) transitions. For Dy(III) complex, three characteristic bands can be seen in the emission spectra (Fig. 9), which are attributed to transitions of 456 nm ($^4I_{15/2} \rightarrow ^6H_{15/2}$) 484 nm ($^4F_{9/2} \rightarrow ^6H_{15/2}$) and 574 nm ($^4F_{9/2} \rightarrow ^6H_{13/2}$). Compared with the emission spectra of the four complexes (Table 5), the relative transition intensity changes in the order of Tb(III) > Eu(III) > Dy(III) > Sm(III).

In addition to steady-state measurements, the luminescence lifetimes of the Sm ($4G_{5/2}$), Eu ($5D_0$), Tb ($5D_4$) and Dy ($4F_{9/2}$) excited

states and quantum yield determinations for Eu, Tb complexes were determined with the results also summarized in Table 5. The relatively long luminescence lifetimes and larger quantum yield values are an indication that the bridging ligand provides a significant level of protection from nonradiative deactivation of lanthanide cations by the solvent molecules. The longer lifetime and the larger quantum yield of Tb(III) than that of Eu(III) is most likely due to the insufficient inter-system crossing (ISC) of Eu(III) complexes, as further supported by the energy transfer discussed below.

To demonstrate the energy transfer process, the phosphorescence spectrum of Gd(III) complex of L was measured for the triplet energy-level data. From the phosphorescence spectra (Fig. 10), the triplet energy level ($^3\pi\pi^*$) of Gd(III) complex, which corresponds to its lower wavelength emission edge, is 25126 cm^{-1} (398 nm). Because the lowest excited state, $^6P_{7/2}$ ($E(^6P_{7/2}) = 32000 \text{ cm}^{-1}$) of Gd(III) is too high to accept energy from the ligand, the data obtained from the phosphorescence spectra actually reveal the triplet

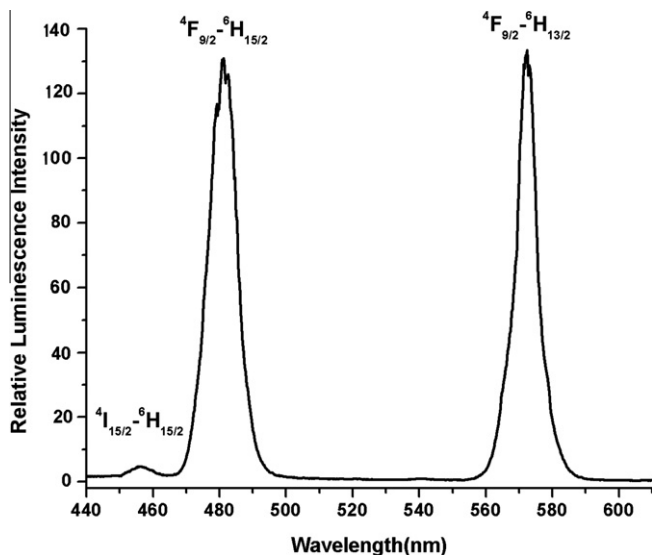


Fig. 9. Room-temperature emission spectra for dysprosium complex of ligand **L** ($\lambda_{\text{exc}} = 320$ nm, excitation and emission passes = 2.5 nm) in the solid state.

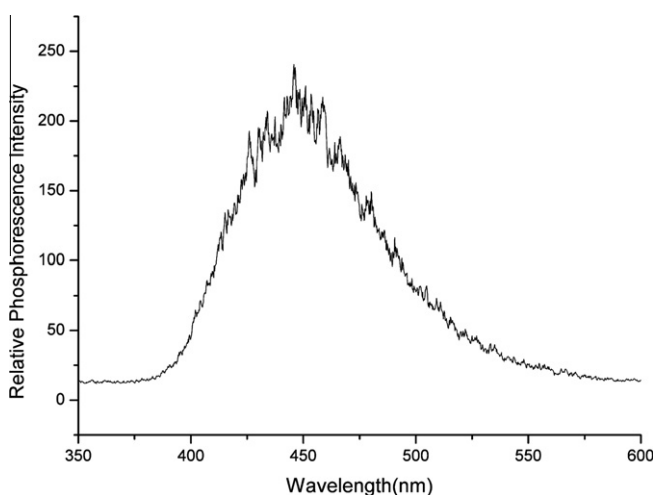


Fig. 10. Phosphorescence spectra of Gd(III) complex of ligand **L** in methanol-ethyl acetate solution at 77 K.

energy level of ligand in lanthanide complexes. In general, the sensitization pathway in luminescent europium complexes consists of excitation of the ligands into their excited singlet states, subsequent intersystem crossing of the ligands to their triplet states and energy transfer from the triplet state to the 5D_J manifold of the Eu(III) ions, followed by internal conversion to the emitting 5D_0 state. Finally, the Eu(III) ion emits when a transition to the ground state occurs [21]. Moreover, electron transition from the higher excited states, such as 5D_3 (24800 cm^{-1}), 5D_2 (21200 cm^{-1}) and 5D_1 (19000 cm^{-1}) to 5D_0 (17500 cm^{-1}) becomes feasible by internal conversion, and most of the photophysical processes take place in this excited states. Consequently, most europium complexes give rise to typical emission bands at ca. 581, 593, 614, 654 and 702 nm, corresponding to the deactivation of the 5D_0 excited state to the 7F_J ground states ($J = 0-4$). In a similar way, the $4f$ electrons of the Tb(III) ion are excited to the 5D_J ion manifold from the ground state. Finally, the Tb(III) ion emits when the $4f$ electrons undergo a transition from the excited state of 5D_4 to the 7F_J ground states ($J = 6-3$). Latva's empirical rule [22] states that an optimal ligand-to-metal energy transfer process for Ln(III) needs $\Delta E = {}^3\pi\pi^* - 5D_J$ (2500–4000 cm^{-1} for Eu(III) and 2500–4500 cm^{-1} for Tb(III)). The

triplet energy level of the salicylamide ligand (25126 cm^{-1}) is higher than the 5D_0 level of Eu(III) (17500 cm^{-1}) and the 5D_4 level of Tb(III) (20400 cm^{-1}). This therefore supports the observation of stronger sensitization of the terbium complexes than the europium complexes because of the smaller overlap between the ligand triplet and europium ion excited states.

For the energy gap between the excited luminescent states and the highest J levels of the ground states of Sm(III) and Dy(III) is ca. 7500 and 7800 cm^{-1} , considerably smaller than that of Eu(III) and Tb(III) with values around 12300 and 14800 cm^{-1} [23]. As a result the lifetime measurements for both the Sm(III) and Dy(III) complexes were found to be 43 and 69 μs , respectively, based on a single-exponential fit of the data, which are much shorter than those observed with Eu(III) or Tb(III) due to the higher water sensitivity [24].

In contrast to Sm(III), Eu(III), Tb(III) and Dy(III) complexes of similar ligands reported previously [11], the lifetimes are shorter slightly, suggesting that one or more nonradiative pathways are assisting in the deactivation of the excited state and shortening the observed lifetimes, since the triplet energy level of the antenna only changed slightly with the backbone group, which excludes the possibility that the quenching of luminescence is due to a change in the nature of the antenna triplet state. The most probable explanation may be the bulky of the backbone which could weaken the coordination bond and thus the efficiency of the energy transfer.

4. Conclusions

We presented here a new semirigid bridging ligand featuring *N*-furfurylamide arms which can form stable coordination polymers with lanthanide nitrates. The coordination polymer $\{\text{Pr}_2(\text{NO}_3)_6\text{L}_3\}_\infty$ displays a two-dimensional honeycomb-like framework in the *ab* plane, which can be regarded as a (6,3) topological network with praseodymium atoms acting as “three-connected” centers. The luminescent properties of the Sm(III), Eu(III), Tb(III) and Dy(III) complexes were investigated in detail. It is worthy noting that the bridging ligand provides a significant level of protection from nonradiative deactivation of lanthanide cations by the solvent molecules and exhibits a good antennae effect with respect to the Tb(III) ion due to efficient intersystem crossing and ligand-to-metal energy transfer. Our present findings provide the possibility of controlling the formation of the desired lanthanide coordination structure to enrich the crystal engineering strategy and enlarges the arsenal for developing excellent luminescent lanthanide complexes of salicylamide derivatives.

Acknowledgment

This work was supported by the National Natural Science Foundation of China (Grant No. 21161011).

Appendix A. Supplementary material

CCDC 863911 contains the supplementary crystallographic data for this paper. These data can be obtained free of charge from The Cambridge Crystallographic Data Centre via www.ccdc.cam.ac.uk/data_request/cif. Supplementary data associated with this article can be found, in the online version, at <http://dx.doi.org/10.1016/j.ica.2012.04.007>.

References

- [1] J.-G.G. Bünzli, S. Comby, A.-S. Chauvin, C.D.B. Vandevyver, J. Rare Earth 25 (2007) 257.
- [2] (a) F.Y. Li, H. Yang, C.H. Huang, Rare Earth Coordination Chemistry (2010) 529; (b) J. Yu, D. Parker, R. Pal, R.A. Poole, M.J. Cann, J. Am. Chem. Soc. 128 (2006) 2294.
- [3] J.-C. Bünzli, C. Piguet, Chem. Soc. Rev. 34 (2005) 1048.

- [4] M. Fernandes, S.S. Nobre, M.C. Goncalves, A. Charas, J. Morgado, R.A.S. Ferreira, L.D. Carlos, V. de Zea Bermudez, J. Mater. Chem. 19 (2009) 733.
- [5] (a) M. Giraud, E.S. Andreiadis, A.S. Fisyuk, R. Demadrille, J. Pécaut, D. Imbert, M. Mazzanti, Inorg. Chem. 47 (2008) 3952;
(b) E.S. Andreiadis, R. Demadrille, D. Imbert, J. Pécaut, M. Mazzanti, Chem.-Eur. J. 15 (2009) 9458.
- [6] F.-Y. Yi, Q. -P Lin, T. -H Zhou, J.-G. Mao, Cryst. Growth. Des. 10 (2010) 1788.
- [7] (a) G.F. de Sá, O.L. Malta, C. de Mello Doneg'a, A.M. Simas, R.L. Longo, P.A. Santa-Cruz, E.F. da Silva Jr., Coord. Chem. Rev. 196 (2000) 165;
(b) P.N. Remya, S. Biju, M.L.P. Reddy, A.H. Cowley, M. Findlater, Inorg. Chem. 47 (2008) 7396;
(c) D.B.A. Raj, B. Francis, M.L.P. Reddy, R.R. Butorac, V.M. Lynch, A.H. Cowley, Inorg. Chem. 49 (2010) 9055;
(d) S. Biju, D.B.A. Raj, M.L.P. Reddy, C.K. Jayasankar, A.H. Cowley, M. Findlater, J. Mater. Chem. 19 (2009) 1425.
- [8] (a) M. Seitz, M.D. Pluth, K.N. Raymond, Inorg. Chem. 46 (2007) 351;
(b) E.G. Moore, C.J. Jocher, J. Xu, E.J. Werner, K.N. Raymond, Inorg. Chem. 46 (2007) 5468;
(c) E.G. Moore, J. Xu, C.J. Jocher, I. Castro-Rodriguez, K.N. Raymond, Inorg. Chem. 47 (2008) 3105;
(d) A.P.S. Samuel, E.G. Moore, M. Melchior, J. Xu, K.N. Raymond, Inorg. Chem. 47 (2008) 7535;
(e) A.P.S. Samuel, J. Xu, K.N. Raymond, Inorg. Chem. 48 (2009) 687.
- [9] A.J. Amoroso, M.W. Burrows, R. Haigh, M. Hatcher, M. Jones, U. Kynast, K.M.A. Malik, D. Sendor, Dalton Trans. 16 (2007) 1630.
- [10] (a) N. Chatterton, Y. Bretonnière, J. Pécaut, M. Mazzanti, Angew. Chem., Int. Ed. 44 (2005) 7595;
(b) G.S. Kottas, M. Mehlstäubl, R. Fröhlich, L. De Cola, Eur. J. Inorg. Chem. 22 (2007) 3465;
(c) L.J. Charbonnière, S. Mameri, D. Flot, F. Waltz, C. Zandanel, R.F. Ziessel, Dalton Trans. 22 (2007) 2245;
(d) L.S. Natrajan, P.L. Timmins, M. Lunn, S.L. Heath, Inorg. Chem. 46 (2007) 10877;
(e) L. Benisvy, P. Gamez, W.T. Fu, H. Kooijman, A.L. Spek, A. Meijerink, J. Reedijk, Dalton Trans. 24 (2008) 3147;
(f) N.M. Shavaleev, F. Gumy, R. Scopelliti, J.-C.G. Bünzli, Inorg. Chem. 48 (2009) 5611;
(g) R. Feng, F.-L. Jiang, M.-Y. Wu, L. Chen, C.-F. Yan, M.-C. Hong, Cryst. Growth. Des. 10 (2010) 2306.
- [11] (a) J. Zhang, Y. Tang, N. Tang, M.-Y. Tan, W.-S. Liu, K.-B. Yu, J. Chem. Soc., Dalton Trans. 14 (2002) 832;
(b) Y. Tang, J. Zhang, W.-S. Liu, M.-Y. Tan, K.-B. Yu, Polyhedron 24 (2005) 1160;
(c) X.-Q. Song, W.-S. Liu, W. Dou, Y.-W. Wang, J.-R. Zheng, Z.-P. Zang, Eur. J. Inorg. Chem. 11 (2008) 1901;
(d) X.-Q. Song, W.-S. Liu, W. Dou, J.-R. Zheng, X.-L. Tang, H.-R. Zhang, D.-Q. Wang, Dalton Trans. 24 (2008) 3582;
(e) X.-Q. Song, W. Dou, W.-S. Liu, Y. -L. Guo, X. -L. Tang, Inorg. Chem. Commun. 10 (2007) 1058;
(f) Y.-W. Wang, Y.-L. Zhang, W. Dou, A.-J. Zhang, W.-W. Qin, W.-S. Liu, Dalton Trans. 39 (2010) 9013;
(g) Q. Wang, X. Yan, H. Zhang, W. Liu, Y. Tang, M. Tan, J. Solid State Chem. 184 (2011) 164;
(h) X.-Q. Song, W.K. Dong, Y.J. Zhang, W.-S. Liu, Luminescence 25 (2010) 328.
- [12] K. Nakagawa, K. Amita, H. Mizuno, Y. Inoue, T. Hakushi, Bull. Chem. Soc. Jpn. 60 (1987) 2037.
- [13] F. Gutierrez, C. Tedeschi, L. Maron, J.-P. Daudey, R. Poteau, J. Azema, P. Tisnès, C. Picard, Dalton Trans. 9 (2004) 1334.
- [14] M.S. Wrighton, D.S. Ginley, D.L. Morse, J. Phys. Chem. 78 (1974) 2229.
- [15] K. Michio, Bull. Chem. Soc. Jpn. 49 (1976) 2679.
- [16] Z. Jiri, P. Magdalena, H. Petr, T. Milos, Synthesis 110 (1994) 1132.
- [17] G.M. Sheldrick, SHELXL-97, Program for Crystal Structure Solution and Refinement, University of Göttingen, Göttingen, Germany, 1997.
- [18] K. Nakamoto, Infrared and Raman Spectra of Inorganic and Coordination Compounds, Wiley, New York, 1978, p. 227.
- [19] M. Albin, R.R. Whittle, W.D. Horrocks Jr., Inorg. Chem. 24 (1985) 4591.
- [20] A.F. Kirby, D. Foster, F.S. Richardson, Chem. Phys. Lett. 95 (1983) 507.
- [21] (a) R. Pavithran, N.S. Saleesh Kumar, S. Biju, M.L.P. Reddy, S. Alves Jr., R.O. Freire, Inorg. Chem. 45 (2006) 2184;
(b) R. Pavithran, M.L.P. Reddy, S. Alves Jr., R.O. Freire, G.B. Rocha, P.P. Lima, Eur. J. Inorg. Chem. 20 (2005) 4129;
(c) M. Shi, F. Li, T. Yi, D. Zhang, H. Hu, C. Huang, Inorg. Chem. 44 (2005) 8929.
- [22] M. Latva, H. Takalo, V.M. Mukkala, C. Matachescu, J.C. Rodriguez-Ubis, J. Kanakare, J. Lumin. 75 (1997) 149.
- [23] S.W. Magennis, S. Parsons, Z. Pikramenou, Chem. Eur. J. 8 (2002) 5761.
- [24] D.R. Lide (Ed.), CRC Handbook of Chemistry and Physics, 80th ed., CRC Press, Boca Raton, FL, 1999.